Published in final edited form as:
Neuropsychology. 2002 July ; 16(3): 370–379.

Working Memory for Complex Figures: An fMRI Comparison of Letter and Fractal *n*-Back Tasks

J. Daniel Ragland, **Bruce I. Turetsky**, **Ruben C. Gur**, **Faith Gunning-Dixon**, **Travis Turner**, **Lee Schroeder**, **Robin Chan**, and **Raquel E. Gur**
University of Pennsylvania School of Medicine

Abstract

n -back letter and fractal tasks were administered to 11 participants during functional magnetic resonance imaging to test process specificity theories of prefrontal cortex (PFC) function and assess task validity. Tasks were matched on accuracy, but fractal *n*-back responses were slower and more conservative. Maintenance (1-back minus 0-back) activated inferior parietal and dorsolateral PFC, with additional activation in right ventrolateral PFC during letter *n*-back and left lingual gyrus during fractal *n*-back. Maintenance plus manipulation (2-back minus 0-back) activated inferior parietal, Broca's area, insula, and dorsolateral and ventral PFC, with greater right dorsolateral PFC activation for letter *n*-back. Manipulation only (2-back minus 1-back) produced additional and equivalent dorsolateral PFC and anterior cingulate activation in both tasks. Results support fractal *n*-back validity and indicate substantial overlap in working memory functions of dorsal and ventral PFC.

Working memory refers to a limited capacity system responsible for temporary maintenance and online manipulation of information required for guidance of subsequent behavior. Working memory is conceptualized as having several components including a central executive system (CES) and two modality-specific slave systems: the visuospatial sketch pad and the phonological loop (Baddeley, 1986, 1992; Baddeley & Hitch, 1974). The CES allocates attentional resources and is responsible for coordination of top–down processes permitting monitoring and manipulation of information within the short-term store (e.g., temporal sequencing). The visuospatial sketch pad maintains visuospatial information in a temporary visuospatial store, and the phonological loop maintains verbal material in a phonological store through an articulatory rehearsal process. Much of the research on working memory has focused on anatomically dissociating these multiple processes. The goal of the current functional magnetic resonance imaging (fMRI) study is to use a parametric *n*-back paradigm (Awh et al., 1996; Braver et al., 1997; Cohen et al., 1994, 1997; Gervins & Cutillo, 1993; Smith, Jonides, & Koeppe, 1996) to contrast the effect of working memory load on regional brain function during a standard letter *n*-back task versus an *n*-back task using complex geometric objects that have not been previously studied.

Correspondence concerning this article should be addressed to: J. Daniel Ragland, 10th Floor Gates Building/HUP, Department of Psychiatry, University of Pennsylvania School of Medicine, Philadelphia, Pennsylvania 19104. ragland@bbl.med.upenn.edu.
J. Daniel Ragland, Bruce I. Turetsky, Ruben C. Gur, Faith Gunning-Dixon, Travis Turner, Lee Schroeder, Robin Chan, and Raquel E. Gur, Department of Psychiatry, University of Pennsylvania School of Medicine.

Demonstrating similar effects of working memory load on the two tasks provides initial evidence for the construct validity of the new task.

The process specificity model attempts to parse prefrontal regions mediating different components of working memory. According to the model, ventrolateral prefrontal cortex (PFC; Brodmann's area [BA] 44, 45, and 47) is responsible for maintenance of information in the visuospatial and phonological stores, and dorsolateral PFC (BA 9 and 46) is required for CES processes of monitoring and manipulation (Petrides, 1994). This model is broadly supported by reviews of human imaging studies of working memory (D'Esposito et al., 1998; Owen, 1997). These studies contrast specific functions (e.g., maintenance vs. maintenance plus monitoring and manipulation) and generally find that ventrolateral PFC mediates maintenance of verbal and non-verbal information and that dorsolateral PFC is involved in executive components of monitoring and manipulation (Berman, Austin-Lane, Esposito, Van Horn, & Weinberger, 1996; Klingberg, O'Sullivan, & Roland, 1997; Manoach et al., 1997; Salmon et al., 1996; Stern et al., 2000; Tsukiura et al., 2001). However, this functional dissociation appears to be relative rather than absolute. For example, Cohen et al. (1997) examined the temporal dynamics of working memory with fMRI and found that dorsolateral PFC activation increased with working memory load and did not decrease over time. This was inconsistent with the assumption that executive processes are transient. These authors concluded that dorsolateral PFC is involved in both maintenance and manipulation. Similarly, D'Esposito, Postle, and Rympa (2000) found sustained activation in both aspects of the PFC for tasks requiring maintenance only and for tasks involving maintenance plus manipulation. Thus, it appears that the dorsolateral PFC is not only involved in executive processes, such as the manipulation and monitoring of information, but also may work in concert with the ventrolateral PFC during active maintenance.

Investigators have also tried to delineate prefrontal regions on the basis of stimulus domain. The domain specificity model is an extension of primate studies linking object identification ("what") with a ventral occipitotemporal pathway and spatial perception ("where") with a dorsal occipitoparietal pathway (Ungerleider & Haxby, 1994; Ungerleider & Mishkin, 1982). On the basis of primate working memory studies using single-cell recordings, the model states that ventrolateral PFC (BA 12 and 45) is involved in working memory for nonspatial material, whereas dorsolateral PFC (BA 46) is involved in working memory for spatial information (Goldman-Rakic, 1995; Wilson, Scalaidhe, & Goldman-Rakic, 1993). Support of domain specificity from the human neuroimaging literature has been inconsistent. Although several studies found prefrontal regions that were differentially activated by working memory for faces versus spatial locations (Courtney, Ungerleider, Keil, & Haxby, 1996; Ungerleider, Courtney, & Haxby, 1998), there was substantial functional overlap (Haxby, Petit, Ungerleider, & Courtney, 2000), and several recent reviews and meta-analyses failed to support domain specificity for dorsal versus ventral aspects of the PFC (D'Esposito et al., 1998; Owen, 1997).

Because the fractal *n*-back task is a measure of object identification (what) rather than of spatial localization (where), the current study could not test domain specificity models of dorsal versus ventral PFC function. However, the current paradigm could test a variant of

the domain specificity model that makes a laterality distinction, claiming a left–right specialization of verbal versus nonverbal working memory functions (Smith & Jonides, 1997). Initial evidence for hemispheric differences in PFC function came from studies contrasting letter versus spatial dot localization tasks (Awh et al., 1996; Jonides et al., 1993; Smith et al., 1996). However, other investigations using spatial working memory tasks did not replicate these earlier findings (D'Esposito et al., 1998; Nystrom et al., 2000). Tests of hemispheric specificity have also been conducted by contrasting working memory for letters with working memory for visual objects. The objects used in these studies have had variable spatial demands (e.g., faces, Korean letters, simple geometric designs) and have produced even less consistent evidence of a hemispheric difference between stimulus domains (Nystrom et al., 2000; Paulesu, Frith, & Frackowiak, 1993; Salmon et al., 1996). A recent study comparing working memory maintenance of famous and unfamous faces versus famous and unfamous names (Rama, Sala, Gillen, Pekar, & Courtney, 2001) found that laterality effects were mediated by whether or not the face was famous. A right–left face versus name dissociation was found only for unfamous faces, leading the investigators to speculate that previous knowledge of famous faces was more likely to invoke both verbal and nonspatial visual processing. Finally, a quantitative review of the literature (D'Esposito et al., 1998) concluded that hemispheric asymmetries might be restricted to ventrolateral PFC rather than dorsolateral PFC.

The *n*-back paradigm is well suited to study both process-specific and domain-specific aspects of the neural correlates of working memory (Awh et al., 1996; Braver et al., 1997; Cohen et al., 1997; Nystrom et al., 2000; Postle, Stern, Rosen, & Corkin, 2000; Smith et al., 1996). During *n*-back tasks, participants view a continuous sequence of stimuli, and for each stimulus, the participants decide whether it matches the stimulus they saw (*n* stimuli) earlier. For example, in the 0-back condition, participants respond to any exposure of a predetermined target; in the 1-back condition, participants respond if the current stimulus matches the stimulus in the previous trial; and in the 2-back condition, participants respond if the current stimulus is the same as the one presented two trials previously. This paradigm can be used to assess process specificity by manipulating memory load to contrast conditions requiring maintenance predominantly (e.g., 1-back) with conditions requiring both maintenance and manipulation (e.g., 2-back). On the basis of previous findings, we hypothesized that although dorsolateral PFC activity increases with increased manipulation demands (i.e., 2-back vs. 1-back), there would be substantial neuroanatomical overlap between dorsal and ventral PFC activity during the maintenance only condition (i.e., 1-back vs. 0-back).

The *n*-back task can also be used with different classes of stimuli to test domain specificity. The current study contrasts a standard letter *n*-back condition (Braver et al., 1997) with an *n*-back task using complex visuospatial fractal stimuli. These geometric stimuli are artificial, cannot be easily labeled, and are designed to meet the need (Haxby et al., 2000) for visual tasks that involve greater levels of spatial perceptual processing than previous object working memory tasks that used faces or line drawings of common objects. Although we did not hypothesize differences in dorsal and ventral PFC function on the basis of stimulus domain, we did hypothesize that the greater spatial demands of processing fractal versus

letter stimuli would be reflected by greater left PFC activity for letter *n*-back and greater right PFC activity for fractal *n*-back.

Materials and Method

Participants

Thirteen healthy volunteers participated. Data from 1 participant were incomplete because of a computer failure, and 1 participant was excluded for excessive movement artifact, leaving a final sample of 11 participants (6 men, 5 women) ranging in age from 21 to 53 years (M = 32.2). Participants had an average of 17 years of education (range = 14 –20 years), and all were right handed on the basis of a standardized inventory (Raczkowski, Kalat, & Nebes, 1974). Participants were free of any present or past disorder or injury that might affect brain function. Informed consent was obtained prior to participation in the study, following procedures approved by the Human Subjects Committee of the University of Pennsylvania School of Medicine.

Tasks

Two versions of an *n*-back working memory task were administered as neurobehavioral probes during fMRI. A letter version of the task was modeled after a standard paradigm (Braver et al., 1997) that was simplified to facilitate its use in future studies of schizophrenia. Briefly, the letter *n*-back task displayed sequences of uppercase consonants with a stimulus duration of 500 ms and an interstimulus interval of 2,500 ms. Uppercase consonants were used to maximize readability of the stimuli. In the 0-back condition, participants responded to a single target (i.e., *X*). During the 1-back condition, participants responded if the consonant was identical to one preceding it. In the 2-back condition, participants responded if the letter was identical to one presented two trials back. A 3-back condition (i.e., response if letter is identical to one presented three trials back) was not used because piloting showed that patients were unable to perform above chance level. There were 15 letters presented for each condition, and each condition was repeated three times in pseudorandom order for a total of 135 stimuli. A target-foil ratio of 1:2 (i.e., 33% targets) was maintained throughout. There was a 9-s delay at the start of the task and between conditions, during which an instruction screen appeared informing the participant of the upcoming condition. This delay also allowed the participant to rest, and it permitted recovery of the hemodynamic response from the previous condition. Total task time was 495 s. The trial sequence is illustrated in Figure 1.

The second task replaced consonants with fractal stimuli but was otherwise identical to the letter *n*-back task. Fractals are complex geometric designs with self-similarity between the small components of the shape and the gestalt of the shape. A natural example is a rocky mountain. From a distance, the mountain outline is rough and jagged. Closer and closer views, down to the surface of the rocks, reveal similar roughness. Fractal stimuli were generated using ArtMatic (1998) software, which assigns random numbers to coordinates in a field, enters the numbers into a formula, and recalculates the formula using thousands of iterations. Twenty different fractal images were used, corresponding to the 20 consonants used in the letter version. Images that were easily named during task development were

excluded. The 0-back, 1-back, and 2-back conditions were generated using the identical parameters and procedures as the letter version of the task. An illustration of the task is provided in Figure 1.

Task administration was triggered by the scanner and coupled to image acquisition using the PowerLaboratory platform (Chute & Westall, 1997) on a Macintosh Powerbook laptop computer. Visual stimuli were presented in the center of the visual field to hold spatial location constant and were viewed through a mirror mounted inside the gantry. Stimuli were rear projected onto a translucent screen perpendicular to participants' feet using an Epson (PowerLite 7300) video projector (Epson Electronics America, Inc., San Jose, CA). Button responses were recorded by way of a color-coded keypad made of nonferromagnetic components (FORP, manufactured by Current Design Inc., Philadelphia, PA). Response hand was randomly assigned, with 3 participants making a right-hand response and 8 participants making a left-hand response. Participants did not all respond with the same hand in order to avoid a consistent bias in the laterality of the motor effects in the group analysis. Practice versions of both tasks were administered to participants before they entered the magnet. To complete the practice, participants had to respond correctly to 11 items in a row. All participants successfully completed practice tasks and did not have any questions about task instructions during the study.

Image Acquisition

Data were acquired on a 4T GE Signa Scanner (General Electric Company, Milwawkee, WI), using a whole-head coil that ran the 5.4 release of the GE Signa scanner software. The 4.0-T system is equipped with a GE quadrature head coil, standard 10-mT/m gradient coils, spectroscopy option and a multicoil option. The system is also equipped with special safety features to protect participants from excess exposure to radiofrequency heating, and a head restraint system designed to control head movement. In its current configuration, the system has met all of GE's normal 1.5 T specifications for stability, image quality, and signal-to-noise ratio. Structural imaging consisted of a sagittal T1-weighted localizer, followed by a T1-weighted acquisition of the entire brain in the axial plane (24 cm FOV, 256 × 256 matrix, resulting in voxel size of 0.9375 × 0.9375 × 4.0000 mm). This sequence was used both for anatomic overlays of the functional data and for spatial normalization of the data sets to a standard atlas (Talairach & Tournoux, 1988). Functional data were obtained using blood oxygenation level dependent (BOLD; Bandettini, Wong, Hinks, Tikofsky, & Hyde, 1992; Kwong et al., 1992) imaging performed in the axial plane using a multislice gradient-echo echo planar sequence with a field of view of 24 (frequency) × 15 (phase) and an acquisition matrix of 64 × 40 (22 slices, 4 mm thickness, no skip, transit time = 2,000, time to echo = 40° and 90° flip angle). This sequence delivers an effective voxel resolution of 3.75 × 3.75 × 4.00 mm. The fMRI raw echo amplitudes were saved and transferred electronically for off-line reconstruction using Interactive Data Language (Research Systems Inc., Boulder, CO). The images were corrected for residual geometric distortion (Jezzard & Balaban, 1995) on the basis of a magnetic field map acquired with a 1-min reference scan performed immediately following acquisition of the T1 localizer (Alsop, 1995). This correction realigns the echoplanar images with the higher quality T1 images used for determining the transformation to the standard atlas.

Data Analysis

Responses were recorded as true positive (TP), false positive (FP), true negative, and false negative. Two primary performance measures were examined. Discriminability (Pr) was calculated as a measure of performance success, and TP RT was calculated as a measure of performance effort. A response bias index (Br) was also calculated to assess response strategy. Pr and Br were calculated following the two-high threshold theory (Snodgrass & Corwin, 1988) that generates statistically independent signal-detection indices. Pr was calculated by subtracting the false-alarm rate [FAR = (FPs + 0.5)/(number of distractors + 1.0)] from the hit rate [HR = (TPs + 0.5)/(number of targets + 1.0)]. Values of 0.5 and 1.0 were added to the numerators and denominators to avoid division by zero. Pr reflects the proportion of time that an individual is either certain that an item is a target or certain that it is a foil and is an index of performance accuracy. Response bias was calculated as follows: Br = FAR/(1.0 − Pr). This represents the proportion of items on which individuals say *yes* when uncertain. A value of 0.5 reflects a neutral bias in which there is a 50/50 chance of saying *yes* or *no* when uncertain. Br values greater than 0.5 indicate a liberal response bias, and values below 0.5 reveal a conservative response bias. RT was measured by calculating the median RT (in milliseconds) for TP responses.

Functional data were preprocessed using MEDx Version 3.3 (2002). Images within each run were motion corrected (Woods, Mazziota, & Cherry, 1993) to the image occurring in the middle of the run. This was done to correct for any motion that might have occurred during an individual task condition (intrarun realignment). Realignment was made to the middle image to minimize the amount of transformation required for images in the last half of the run. The realignment algorithm consisted of a rigid body six-parameter transformation, using a least squares cost function with scaling of intensity. Proportional scaling of each image to its mean can result in white matter activation artifact. Therefore, the images were globally scaled to the mean of voxels not found significantly correlated with the task (Jesper & Andersson, 1997). This mask was created by thresholding an intermediate omnibus F-map ($p > .01$). This preliminary statistical analysis, identical to the model described below, was performed on a set of temporary images created by band pass filtering and by smoothing the motion corrected images. After this scaling procedure, the images were band pass filtered (Butterworth, 6 – 80 s) and smoothed (12 mm FWHM, isotropic). The smoothing kernel was based on three times the in-plane resolution at which the data were acquired and was chosen to optimize sensitivity (Hopfinger, Buchel, Holmes, & Friston, 2000) and to account for between-subjects differences in anatomy. Transformation to Talairach space (Talairach & Tournoux, 1988) occurred in two steps. The first transformation was created using a surface registration method (Pelizzari, Chen, Spelbring, Weichselbaum, & Chen, 1989). Contours were hand drawn on the reference image used in the intrarun realignment and on the T1 axial localizer. A least squares fitting algorithm then registered the raw functional image to the localizer. This step accounted for possible movement between the time of acquisition of the localizer image and the functional data. The second transformation was created by hand selecting commissural landmarks on the T1 localizer and using a polynomial Talairach transform with trilinear interpolation.

A multisubject analysis was performed using a two-stage random-effects approach. The random-effects model takes into account intersubject variance in generating the group maps, permitting population-level inferences. In the first stage, a multiple linear regression procedure estimated the hemodynamic response to stimuli at each voxel for each participant. The design matrix included a boxcar waveform convolved with a sample hemodynamic response as implemented in Statistical Parametric Mapping 99 software (Friston et al., 1995a, 1995b). In the second stage, the first stage regression coefficients were treated as data and analyzed using paired *t* tests, contrasting the group of participants at each voxel between two conditions. This image-based analysis was performed for three contrasts: 1-back minus 0-back, 2-back minus 0-back, and 2-back minus 1-back. Contrasts were performed both within and between tasks. Within-task contrasts were performed on the whole brain. Between-task comparisons for each contrast were restricted to voxels that had above-threshold responses for either task during their respective within-task contrasts. This conservative approach ensured that between-task contrasts were limited to hypothesized regions showing reliable task-related activations. Resulting SPM{*T*}s were transformed to the unit normal distribution SPM{*Z*}. SPM{*Z*} were Bonferroni corrected ($Z = 3.6$, $p < .05$, corrected) for the number of resels in the brain (Worsley, Evans, Marrett, & Neelin, 1992) using the theory of Gaussian fields (Friston, Jezzard, & Turner, 1994; Friston, Worsley, Frackowiak, Mazziotta, & Evans, 1994).

Results

Performance

All participants successfully completed both letter and fractal *n*-back tasks. Figure 2 presents Pr (top graph) and RT data (bottom graph). Pr values were entered into a repeated measures analysis of variance (ANOVA; Proc GLM, general linear procedure; SAS Institute, 1996) to examine main effects of task (letter, fractal), load (0-back, 1-back, 2-back), and the interaction between task and load. The analysis revealed a main effect of load, $F(2, 9) = 4.6$, $p < .05$, but no effect of task, $F(1, 10) = 2.5$, $p > .05$, or any Task × Load interaction, $F(2, 9) = 2.8$, $p > .05$. Thus, performance decreased with increasing working memory load, but there was no difference in performance accuracy between letter and fractal tasks. The ANOVA was also performed using median RT as a measure of performance speed and effort. In this analysis, there was an effect of task, $F(1, 10) = 10.5$, $p < .01$, an effect of load at a trend level, $F(2, 9) = 3.6$, $p = .06$, and no interaction, $F(2, 9) = 2.4$, $p > .05$. As can be seen in Figure 2, RTs were somewhat longer for the fractal task and tended to increase with increasing working memory load. When debriefed after the study, participants consistently reported trying to form verbal descriptions of the fractal stimuli despite the task being designed as a nonlinguistic task. This may help explain the increased RT in contrast to the letter stimuli that required rapid over-learned letter identification processes.

Results for the Br were more complex. The ANOVA revealed main effects of task, $F(1, 10) = 22.8$, $p < .01$; load, $F(2, 9) = 4.8$, $p < .05$; and Task × Load interaction, $F(2, 9) = 7.3$, $p < .05$. As can be seen in Figure 3, the task effect was due to participants having a more conservative response bias across conditions on the fractal task (Br = 0.29 ± 0.05 vs. 0.35 ± 0.06). The effect of load revealed a tendency for responses to become more conservative

with increasing load. Finally, the interaction between task and load reflected a more conservative bias for the 2-back condition in the fractal task (Br = 0.20 ± 0.04 vs. 0.40 ± 0.05), $F(1, 10) = 11.0$, $p < .01$, with no difference between fractal and letter tasks in either 0-back (Br = 0.40 ± 0.02 vs. 0.34 ± 0.00), $F(1, 10) = 0.9$, $p > .05$, or 1-back conditions (Br = 0.30 ± 0.03 vs. 0.33 ± 0.01), $F(1, 10) = 1.5$, $p > .05$. Participants were less likely to respond when unsure during the fractal task, particularly at the highest working memory load. Thus, although letter and fractal tasks were matched on performance accuracy, slower RTs and a more conservative response style suggest that the fractal task may have been somewhat more difficult.

Regional Cerebral Blood Flow Change

The 1-back minus 0-back contrast—This contrast was designed to reveal fMRI changes related to working memory maintenance while minimizing demands on the CES and controlling for perceptual and motor components. Results for the two tasks are illustrated in Figure 4 and Table 1. Both tasks activated the inferior parietal cortex (BA 40) that is believed to house temporary information stores used by phonological loop and visuospatial sketch pad systems to maintain information in working memory (Paulesu et al., 1993; Salmon et al., 1996). Contrary to hemispheric laterality theories of domain specificity (Smith & Jonides, 1997), there was no clear left–right dissociation of letter and fractal maintenance in the parietal cortex (i.e., bilateral letter activation, left hemisphere fractal activation). Results also ran counter to the process specificity model, as both tasks activated the dorsolateral PFC, with right hemisphere effects for the letter task (BA 9) and left hemisphere effects for the fractal task (BA 46). The letter *n*-back showed an additional area of activation in the right ventrolateral PFC (BA 45), and the fractal task showed additional activation in the left lingual gyrus (BA 19). However, when contrasts were performed directly comparing 1-back minus 0-back activations between the two tasks, there were no differences in regional activation.

The 2-back minus 0-back contrast—This contrast was designed to reveal fMRI changes reflecting the addition of CES components (monitoring and manipulation) to on-line maintenance demands. As can be seen in Figure 5 (and Table 2), both tasks again activated bilateral inferior parietal regions (BA 40) and the right dorsolateral PFC (BA 9 and 46). Both tasks also produced activation in left Broca's area (BA 44), which is a region believed to mediate articulatory rehearsal during operation of the phonological loop (Awh et al., 1996; Paulesu et al., 1993). The right insula was also activated by both tasks, as was a more ventral aspect of the PFC (BA 46 and 10) that showed right hemisphere activation for the letter task and left hemisphere effects for the fractal task. The letter task showed an additional area of activation in the right middle temporal gyrus (BA 21 and 37), and the fractal task showed additional effects in the left insula, left middle frontal gyrus (BA 46), and the anterior cingulate (BA 32). When results for the two tasks were directly contrasted (see Table 2 and Figure 5), dorsolateral PFC activity (BA 9 and 46) was higher for the letter *n*-back task in the right hemisphere. The fractal task did not show any areas of greater activation.

The 2-back minus 1-back contrast—The final contrast was intended to remove the effect of maintenance demands shared by 1-back and 2-back tasks and to isolate fMRI effects of the increased executive demands of the 2-back condition. These results are illustrated in Figure 6 (and Table 3). In accordance with the process specificity model, there was increased dorsolateral PFC activation for both letter (left BA 46, right BA 9 and 10) and fractal tasks (right BA 9 and 46). However, this effect was not restricted to dorsal regions, and PFC activation extended to left ventrolateral (BA 10) and premotor areas (BA 44 and 6) for the fractal task. Additional areas of activation during the letter task included bilateral insula and left thalamus. Both tasks also activated the anterior cingulate (BA 32). Anterior cingulate activation has been previously associated with executive components of working memory (D'Esposito et al., 1995) and is most commonly attributed to mediation of response selection and attentional processing (Posner & Petersen, 1990). As in previous contrasts, the inferior parietal cortex (BA 40) was also activated, with bilateral effects for the letter task and left hemisphere effects for the fractal task. When results for the two tasks were directly contrasted, there were no differences in regional activation.

Discussion

The current study used a parametric *n*-back design to examine the impact of memory load on working memory for visually presented letters versus complex geometric designs. Tasks were successfully balanced on performance accuracy, and performance decreased and RT increased with increased load. Both tasks showed similar effects of increased memory load; however, neither task provided unequivocal support for the process specificity model. Although there was evidence of increased dorsolateral PFC activation in the condition of highest memory load when CES monitoring and manipulation demands were greatest (i.e., 2-back minus 1-back contrast), the dorsolateral PFC was also activated during a 1-back condition that is typically classified as a maintenance only task (Nystrom et al., 2000).

These results converge with recent findings to suggest that the locus of human PFC function during working memory does not clearly segregate with degree of executive processing. Despite consistent support for the conclusion that dorsolateral PFC activation is related to operation of the CES (D'Esposito et al., 1998; Stern et al., 2000), other working memory studies have also shown activation of the dorsolateral PFC during maintenance only tasks (Nystrom et al., 1998; Rypma, Prabhakaran, Desmond, Glover, & Gabrieli, 1999). These combined results have precipitated a return to the view of the human PFC as a complex multi-modal area with diverse reciprocal inputs (Fuster, 1997; Nauta, 1971) that does not clearly segregate along simple dimensions in the same way that posterior cortical areas mediate object versus spatial perception (Cohen, Braver, & O'Reilly, 1996). This revised theoretical framework notes that although there may be some amount of regional specialization, functional roles of dorsal and ventral portions of the PFC vary by degree and are not orthogonal (Haxby et al., 2000; Miller, 2000; Nystrom et al., 2000).

In contrasting letter and fractal *n*-back tasks, we also planned to test hemispheric models of domain specificity. Fractal stimuli were constructed as complex visual designs that were difficult to name. We, therefore, hypothesized that the fractal stimuli would require a greater degree of spatial processing and would produce greater right PFC activity than the letter

task. Paradoxically, it appears that making the fractal stimuli more difficult to name resulted in participants increasing their effort to form verbal representations. Participants reported trying to use verbal strategies, and longer RTs on the fractal task likely reflect the increased effort of forming these representations rather than the more automatic process of letter identification. This resulted in few hemispheric differences when tasks were directly contrasted. In one contrast (2-back minus 0-back), there was evidence of greater right dorsolateral PFC activation during the letter task. Presenting the letters in uppercase form only may have encouraged spatial processing and contributed to this finding.

These unexpected laterality results and the tendency of participants to verbally process the fractal stimuli illustrate the human propensity to process information verbally regardless of stimulus features and may help explain why there has been inconsistent support for the hemispheric model of domain specificity. For example, in a series of three *n*-back studies directly contrasting letters, shapes, and spatial locations, Nystrom and colleagues (2000) could not identify any single region that activated to one stimulus type only. One strategy for counteracting the human propensity for verbal processing is to use articulatory suppression techniques. This was done in a study of object versus spatial working memory (Nystrom et al., 2000) in which participants read aloud during the memory delays to suppress articulatory rehearsal. However, despite this procedure, there was still not a clear region by domain dissociation in the PFC. As early as 1980 (Gur & Reivich, 1980), Ruben C. Gur noted that physiologic evidence of hemispheric dominance has never approached the uniformity of findings that can be obtained from clinical data and split-brain studies. This led to an investigation of individual differences (e.g., sex, handedness, right vs. left conjugate lateral eye “movers”) that demonstrated great individual variability in cerebral blood flow laterality and verbal and spatial task performance. Participants who were more likely to rely on verbal cognitive strategies (e.g., “right movers”) had worse spatial performance and showed a left hemisphere dominance across tasks. These combined findings illustrate the need to take the individual characteristics of a research sample into account and to take caution against simple and invariant hemispheric dichotomies between verbal and spatial tasks.

This study was performed at a high-field strength (4.0 T). Even though high fields can increase susceptibility artifact (particularly in ventral regions such as orbitofrontal cortex), they also offer several advantages over lower field imaging. Although shorter echo times and shorter echo trains are usually required at high field, the larger fractional signal change (Turner et al., 1993) and the higher intrinsic signal-to-noise ratio at 4.0 T make higher field BOLD imaging more sensitive than 1.5 T (Gati, Menon, Ugurbil, & Rutt, 1997). It has also been argued that lower field strength imaging is primarily sensitive to large veins, whereas the capillary level changes, which have improved spatial resolution, can only be detected with high-field imaging (Menon, Ogawa, Tank, & Ugurbil, 1993). Experiences from previous collaborators on our low- and high-field magnets suggest a factor of between two and three in sensitivity for similar protocols at 1.5 and 4.0 T (Maldjian, Gottschalk, Patel, Detre, & Alsop, 1999a; Maldjian et al., 1999b). However, snapshot echoplanar images can suffer from severe geometric distortion. Therefore, a phase encoded reference scan was acquired prior to BOLD imaging to provide both ghost elimination and distortion correction

(Alsop, 1995). This method has permitted us to detect reliable task-related activation in regions subject to increased artifact such as the amygdala (Gur et al., in press). Therefore, it is unlikely that increased susceptibility artifact interfered with our ability to study dorsolateral and ventrolateral PFC regions in the current study.

Finally, these results support the use of fractal stimuli in future *n*-back studies of working memory in healthy participants and patients with schizophrenia. Performance accuracy is the same as in standard letter *n*-back paradigms, and performance is sensitive to parametric manipulations of memory load. fMRI results indicate that the fractal *n*-back task is sensitive to changes in memory load and that it successfully activates a standard network of working memory regions including dorsal and ventral PFC, inferior parietal cortex, Broca's area, insula, anterior cingulate, and premotor areas.

Acknowledgments

This research was supported by the EJLB Foundation and by National Institutes of Health Grants MH-19112, MH-00586, MH-48539, MH 43880, and M01RR0040. We thank Shannan Smith and Miriam Trelka for assistance with participant accrual and Alexis Perkins, Norman Butler, and the staff of HUP6 for assistance in data collection.

References

Alsop DC. Correction of ghost artifacts and distortion in echoplanar MR imaging with an iterative reconstruction technique. Radiology. 1995; 197:388.

ArtMatic. Statistics software [Computer software]. 1998. Retrieved from http://www.artmatic.com

Awh E, Jonides J, Smith EE, Schumacher EH, Koeppe RA, Katz S. Dissociation of storage and rehearsal in verbal working memory: Evidence from PET. Psychological Science. 1996; 7:25–31.

Baddeley, AD. Working memory. Oxford, England: Oxford University Press; 1986.

Baddeley AD. Working memory. Science. 1992 Jan 31.255:556–559. [PubMed: 1736359]

Baddeley, AD.; Hitch, GJ. Working memory. In: Bower, GA., editor. The psychology of learning and motivation. Vol. 8. New York: Academic Press; 1974. p. 47-89.

Bandettini PA, Wong EC, Hinks RS, Tikofsky RS, Hyde JS. Time course of EPI of human brain function during task activation. Magnetic Resonance in Medicine. 1992; 25:390–397. [PubMed: 1614324]

Berman KF, Austin-Lane JL, Esposito G, Van Horn JD, Weinberger DR. Dissecting the "working" and the "memory" in a PET study of working memory using graded tasks and isomorphic stimuli. NeuroImage. 1996; 3:S529.

Braver TS, Cohen JD, Nystrom LE, Jonides J, Smith EE, Noll CD. A parametric study of prefronal cortex involvement in human working memory. NeuroImage. 1997; 5:49–62. [PubMed: 9038284]

Chute, DL.; Westall, RF. PowerLaboratory. Devon, PA: MacLaboratory; 1997.

Cohen JD, Braver TS, O'Reilly R. A computational approach to prefrontal cortex, cognitive control, and schizophrenia: Recent developments and current challenges. Philosophical Transactions of the Royal Society of London. 1996; 351:1515–1527. [PubMed: 8941963]

Cohen JD, Forman SD, Braver TS, Casey BJ, Servan-Schreiber D, Noll DC. Activation of prefrontal cortex in a nonspatial working memory task with functional MRI. Human Brain Mapping. 1994; 1:293–304. [PubMed: 24591198]

Cohen JD, Perlstein WM, Braver TS, Nystrom LE, Noll DC, Jonides J, Smith EE. Temporal dynamics of brain activation during a working memory task. Nature. 1997 Apr 10.386:604–608. [PubMed: 9121583]

Courtney SM, Ungerleider LG, Keil K, Haxby JV. Object and spatial visual working memory activate separate neural systems in human cortex. Cerebral Cortex. 1996; 6:39–49. [PubMed: 8670637]

D'Esposito M, Aguirre GD, Zarahn E, Ballard D, Shin RK, Lease J. Functional MRI studies of spatial and non-spatial working memory. Cognitive Brain Research. 1998; 7:1–13. [PubMed: 9714705]

D'Esposito M, Detre JA, Alsop DC, Shin RK, Atlas S, Grossman M. Functional MRI studies of spatial and nonspatial working memory. Cognitive Brain Research. 1995; 7:1–13. [PubMed: 9714705]

D'Esposito M, Postle BR, Rympa B. Prefrontal cortical contributions to working memory: Evidence from event-related studies. Experimental Brain Research. 2000; 133:3–11. [PubMed: 10933205]

Friston KJ, Ashburner J, Frith CD, Poline JB, Heather JD, Frackowiak RSJ. Spatial registration and normalization of images. Human Brain Mapping. 1995a; 2:165–189.

Friston KJ, Holmes AP, Worsley KJ, Poline JP, Frith CD, Frackowiak RSJ. Statistical parametric maps in functional imaging: A general linear approach. Human Brain Mapping. 1995b; 2:189–210.

Friston KJ, Jezzard P, Turner R. Analysis of functional MRI time-series. Human Brain Mapping. 1994; 1:153–171.

Friston KJ, Worsley KJ, Frackowiak RSJ, Mazziotta JC, Evans AC. Assessing the significance of focal activations using their spatial extent. Human Brain Mapping. 1994; 1:210–220. [PubMed: 24578041]

Fuster, JM. The prefrontal cortex: Anatomy, physiology and neuropsychology of the frontal lobe. 3. New York: Lippincott-Raven; 1997.

Gati JS, Menon RS, Ugurbil K, Rutt BK. Experimental determination of the BOLD field strength dependence in vessels and tissue. Magnetic Resonance Medicine. 1997; 38:296–302.

Gervins AS, Cutillo BC. Neuroelectric evidence for distributed processing in human working memory. Electroencephalography and Clinical Neurophysiology. 1993; 87:128–143. [PubMed: 7691540]

Goldman-Rakic PS. Architecture of the prefrontal cortex and the central executive. Proceedings of the National Academy of Sciences, USA. 1995; 769:71–83.

Gur RC, Reivich M. Cognitive task effects on hemispheric blood flow in humans: Evidence for individual differences in hemispheric activation. Brain and Language. 1980; 9:78–92. [PubMed: 7357384]

Gur RC, Schroeder L, Turner T, McGrath C, Chan RM, Turetsky BI, et al. Brain activation during facial emotion processing. NeuroImage. in press.

Haxby JV, Petit L, Ungerleider LG, Courtney SM. Distinguishing the functional roles of multiple regions in distributed neural systems for visual working memory. NeuroImage. 2000; 11:380–391. [PubMed: 10806025]

Hopfinger JB, Buchel C, Holmes AP, Friston KJ. A study of analysis parameters that influence the sensitivity of event-related fMRI analyses. NeuroImage. 2000; 11:326–333. [PubMed: 10725188]

Jesper LR, Andersson JLR. How to estimate global activity independent of changes in local activity. NeuroImage. 1997; 6:237–244. [PubMed: 9453855]

Jezzard P, Balaban RS. Correction for geometric distortion in echo planar images from B0 field variations. Magnetic Resonance in Medicine. 1995; 34:65–73. [PubMed: 7674900]

Jonides J, Smith EE, Koeppe RA, Awh E, Minoshima S, Mintun MA. Spatial working memory in humans as revealed by PET. Nature. 1993 Jun 17.363:623–625. [PubMed: 8510752]

Klingberg T, O'Sullivan BT, Roland PE. Bilateral activation of fronto-parietal networks by incremental demand in a working memory task. Cerebral Cortex. 1997; 7:465–471. [PubMed: 9261575]

Kwong K, Belliveau JW, Chesler DA, Goldberg IE, Weisskoff RM, Poncelet BP, et al. Dynamic magnetic resonance imaging of human brain activity during primary sensory stimulation. Proceedings of the National Academy of Sciences, USA. 1992; 89:5675–5679.

Maldjian JA, Gottschalk A, Patel RS, Detre JA, Alsop DC. The sensory somatotopic map of the human hand demonstrated at 4 tesla. NeuroImage. 1999a; 10:55–62. [PubMed: 10385581]

Maldjian JA, Gottschalk A, Patel RS, Pincus D, Detre JA, Alsop DC. Mapping of secondary somatosensory cortex activation induced by vibrational stimulation: An fMRI study. Brain Research. 1999b; 824:291–295. [PubMed: 10196461]

Manoach DS, Schlaug G, Siewart B, Darby DG, Bly BM, Benfield A, et al. Prefrontal cortex fMRI signal changes are correlated with working memory load. NeuroReport. 1997; 8:545–549. [PubMed: 9080445]

MEDx software (Version 3.3) [Computer software]. Sterling, VA: Sensor Systems, Inc; 2002.

Menon RS, Ogawa S, Tank DW, Ugurbil K. Tesla gradient recalled echo characteristics of photic stimulation-induced signal changes in the human primary visual-cortex. Magnetic Resonance Medicine. 1993; 30:380–386.

Miller EK. The prefrontal cortex: No simple matter. NeuroImage. 2000; 11:447–450. [PubMed: 10806030]

Nauta WJH. The problem of the frontal lobe: A reinterpretation. Journal of Psychiatric Research. 1971; 8:167–187. [PubMed: 5000109]

Nystrom LE, Braver TS, Sabb FW, Delgado MR, Noll DC, Cohen JD. Dynamics of fMRI: Broca's area activation reflects independent effects of duration and intensity of working memory processes. NeuroImage. 1998; 7:S7.

Nystrom LE, Braver TS, Sabb FW, Delgado MR, Noll DC, Cohen JD. Working memory for letters, shapes and locations: fMRI evidence against stimulus-based regional organization of human prefrontal cortex. NeuroImage. 2000; 11:424–446. [PubMed: 10806029]

Owen AM. The functional organization of working memory processes within the human lateral frontal cortex: The contribution of functional neuroimaging. European Journal of Neuroscience. 1997; 9:1329–1339. [PubMed: 9240390]

Paulesu E, Frith CD, Frackowiak RS. The neural correlates of the verbal component of working memory. Nature. 1993 Mar 25.362:342–345. [PubMed: 8455719]

Pelizzari CA, Chen GT, Spelbring DR, Weichselbaum RR, Chen CT. Accurate three-dimensional registration of CT, PET and/or MR images of the brain. Journal of Computer Assisted Tomography. 1989; 8:20–26. [PubMed: 2492038]

Petrides, M. Frontal lobes and working memory: Evidence from investigations of the effects of cortical excisions in non-human primates. In: Boller, R.; Gradfman, J., editors. Handbook of neuropsychology. Amsterdam: Elsevier Science; 1994. p. 59-84.

Posner MI, Petersen SE. The attentional system of the human brain. Annual Reviews in Neuroscience. 1990; 13:25–42.

Postle BR, Stern CE, Rosen BR, Corkin S. An fMRI investigation of cortical contributions to spatial and non-spatial visual working memory. NeuroImage. 2000; 11:409–423. [PubMed: 10806028]

Raczkowski D, Kalat J, Nebes R. Reliability and validity of some handedness questionnaire items. Neuropsychologia. 1974; 12:43–48. [PubMed: 4821188]

Rama P, Sala JB, Gillen JS, Pekar JJ, Courtney SM. Dissociation of the neural systems for working memory maintenance of verbal and nonspatial visual information. Cognitive, Affective, & Behavioral Neuroscience. 2001; 1:161–171.

Rypma B, Prabhakaran V, Desmond JE, Glover GH, Gabrieli JDE. Load-dependent roles of frontal brain regions in the maintenance of working memory. NeuroImage. 1999; 9:216–226. [PubMed: 9927550]

Salmon E, Van der Linden F, Collette G, Delfiore P, Maquet C, Degueldre C, et al. Regional brain activity during working memory tasks. Brain. 1996; 119:1617–1625. [PubMed: 8931584]

SAS Institute Inc. SAS/STAT Software (Version 6.12) [Computer software]. Cary, NC: Author; 1996.

Smith EE, Jonides J. Working memory: A view from neuroimaging. Cognitive Psychology. 1997; 33:5–42. [PubMed: 9212720]

Smith EE, Jonides J, Koeppe RA. Dissociating verbal and spatial working memory using PET. Cerebral Cortex. 1996; 6:11–20. [PubMed: 8670634]

Snodgrass JG, Corwin J. Pragmatics of measuring recognition memory: Applications to dementia and amnesia. Journal of Experimental Psychology: General. 1988; 117:34–50. [PubMed: 2966230]

Stern CE, Owen AM, Tracey I, Look RB, Rosen BR, Petrides M. Activity in ventrolateral and mid-dorsolateral prefrontal cortex during nonspatial visual working memory processing: Evidence from functional magnetic resonance imaging. NeuroImage. 2000; 11:392–399. [PubMed: 10806026]

Talairach, J.; Tournoux, P. Co-planar stereotaxic atlas of the human brain: 3-dimensional proportional system—An approach to cerebral imaging. New York: Thieme Medical Publishers; 1988.

Tsukiura T, Fujii T, Takahashi T, Xiao R, Inase M, Iijima T, et al. Neuroanatomical distinction between manipulating and maintaining processes involved in verbal working memory: A functional MRI study. Cognitive Brain Research. 2001; 11:13–21. [PubMed: 11240107]

Turner R, Jezzard P, Wen H, Kwong KK, LeBihan D, Zeffiro T, Balaban RS. Function mapping of the human visual cortex at 4 and 1.5 telsa using deoxygenation contrast EPI. Magnetic Resonance Medicine. 1993; 29:277–279.

Ungerleider LG, Courtney SM, Haxby JV. A neural system for human visual working memory. Proceedings of the National Academy of Sciences, USA. 1998; 95:883–890.

Ungerleider LG, Haxby JV. “What” and “where” in the human brain. Current Opinions on Neurobiology. 1994; 4:157–165.

Ungerleider, LG.; Mishkin, M. Two cortical visual systems. In: Ingle, DJ.; Goodale, MA.; Mansfield, RJW., editors. Analysis of visual behavior. Cambridge, MA: MIT Press; 1982. p. 549-586.

Wilson FA, Scalaidhe SP, Goldman-Rakic PS. Dissociation of object and spatial processing domains in primate prefrontal cortex. Science. 1993 Jun 25.260:955–958.

Woods, RP.; Mazziota, JC.; Cherry, SR. Automated image registration. In: Uemura, K., editor. Quantification of brain function: Tracer kinetics and image analysis in brain PET. Amsterdam: Elsevier Science; 1993. p. 391-398.

Worsley KJ, Evans AC, Marrett S, Neelin P. A three-dimensional statistical analysis for rCBF activation studies in the human brain. Journal of Cerebral Blood Flow & Metabolism. 1992; 12:900–918. [PubMed: 1400644]

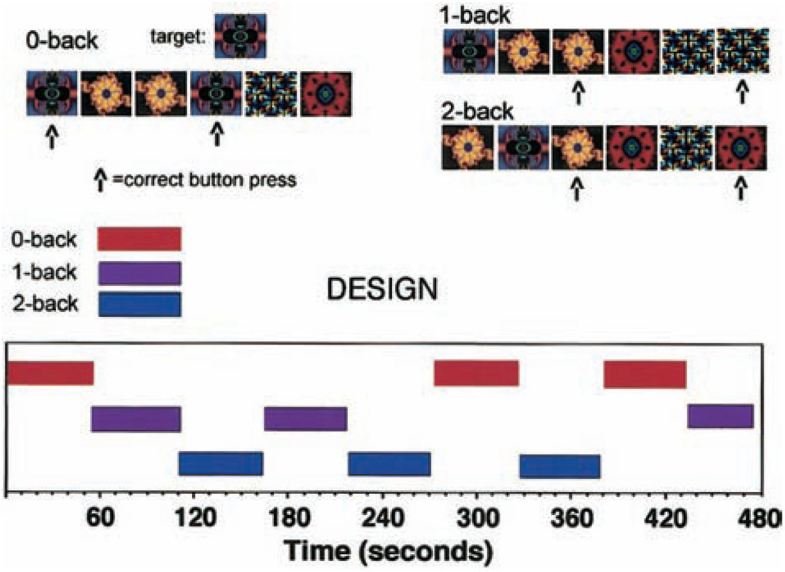

Figure 1.

Illustration of the fractal *n*-back task stimuli and the blocked functional magnetic resonance imaging design.

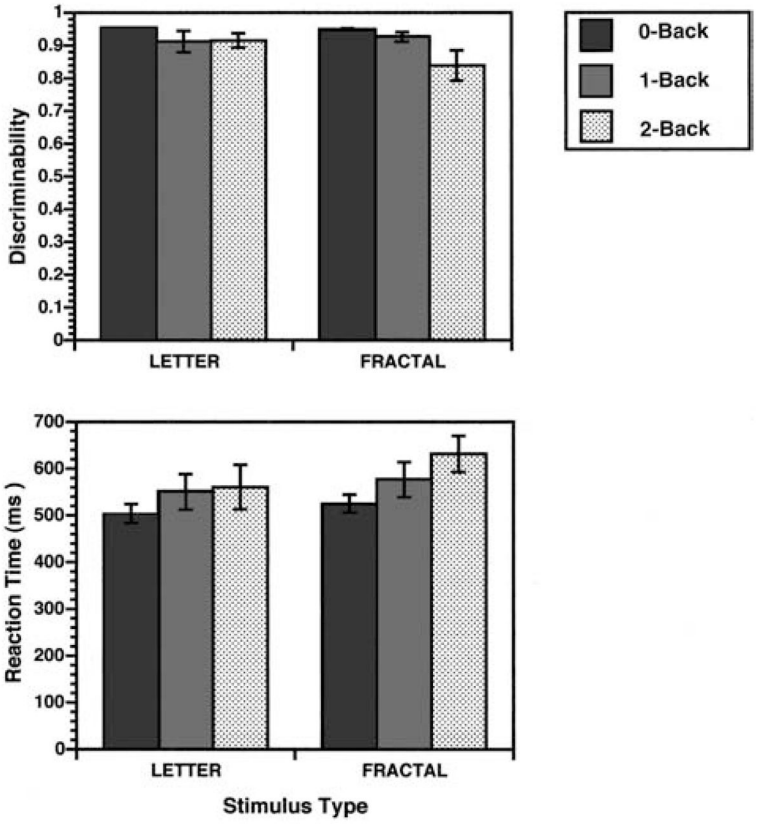

Figure 2.

Mean (±*SEM*) recognition discriminability (top graph) and median reaction time (bottom graph) for 0-back, 1-back, and 2-back conditions for the letter and fractal *n*-back tasks. Discriminability was calculated as an index of recognition accuracy following the two-high threshold model (Snodgrass & Corwin, 1988).

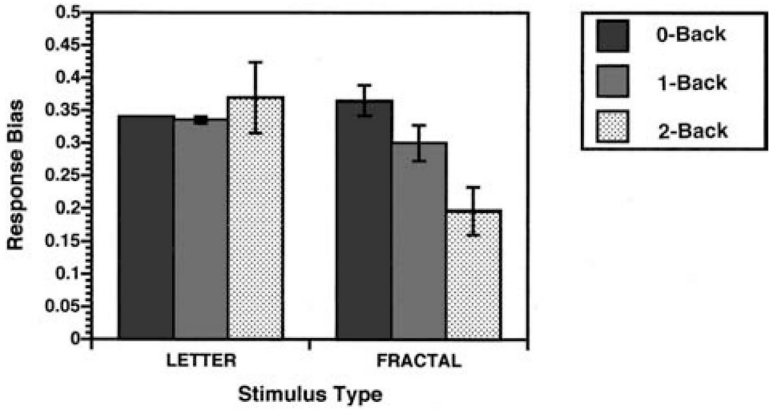

Figure 3.

Mean (±*SEM*) recognition response bias for 0-back, 1-back, and 2-back conditions for the letter and fractal *n*-back tasks. Response bias was calculated following the two-high threshold model (Snodgrass & Corwin, 1988). Values above 0.5 indicate a liberal response bias (i.e., a tendency to respond *yes* to items when unsure), and values below 0.5 indicate a conservative response bias (i.e., a tendency to respond *no* when unsure).

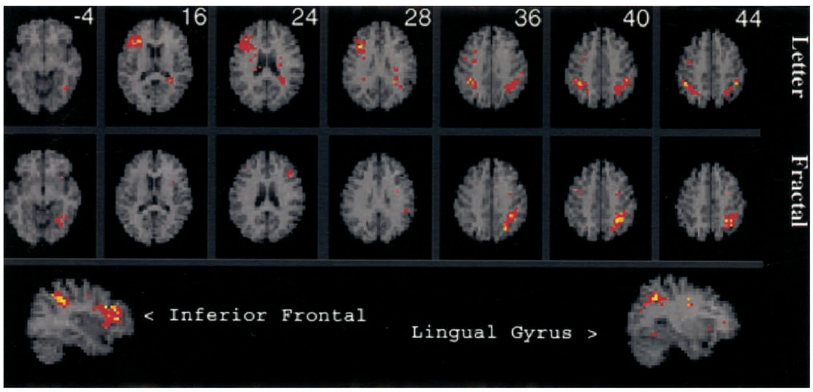

Figure 4.

SPM{*Z*} showing areas activated by 1-back working memory after subtraction of the 0-back condition for the letter *n*-back (top row) and fractal *n*-back (middle row). Sagittal views of letter *n*-back inferior frontal activation and fractal *n*-back lingual gyrus activation are presented in the bottom row. The figure is displayed on an axial and sagittal 4-mm magnetic resonance image that is standardized into Talairach space (Talairach & Tournoux, 1988) and presented in neurologic convention (left is right). Distance from the anterior–posterior commissural plane is indicated for each slice. Colored areas exceed a corrected *p* value of . 05.

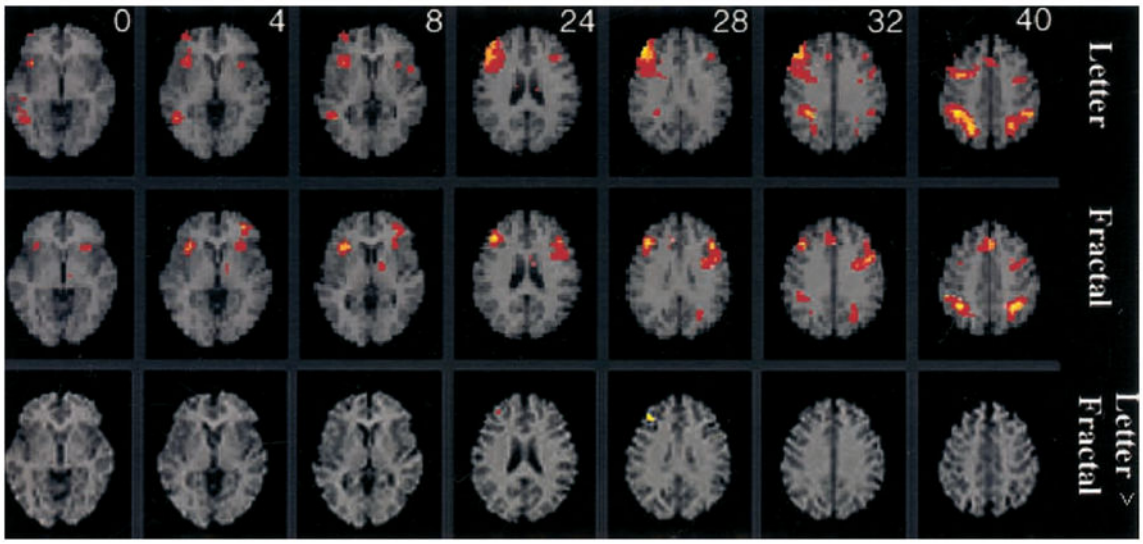

Figure 5.

SPM{*Z*} showing areas activated by 2-back working memory after subtraction of the 0-back condition for the letter *n*-back (top row), fractal *n*-back (middle row), and letter minus fractal *n*-back (bottom row). The same axial display format as Figure 4 is used, with distance from the anterior–posterior commissural plane indicated for each slice.

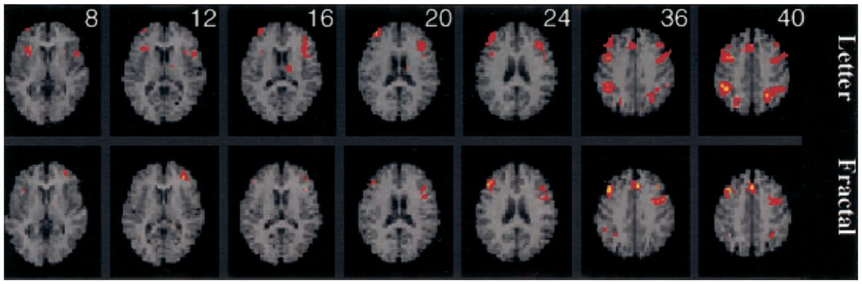

Figure 6.

SPM{*Z*} showing areas activated by 2-back working memory after subtraction of the 1-back condition for the letter *n*-back (top row) and fractal *n*-back (bottom row). The same axial display format as Figure 4 is used, with distance from the anterior–posterior commissural plane indicated for each slice.

Table 1

Local Maxima of Cerebral Blood Flow Change During 1-Back Minus 0-Back

Task and region	Hem	BA	*x*	*y*	*z*	*Z* score
Letter *n*-back						
Inferior frontal	R	45	36	22	16	4.7
Middle frontal	R	9	36	18	28	5.1
Precentral	R	6	28	−6	36	4.4
Inferior parietal	R	40	36	−42	36	5.2
Inferior parietal	L	40	−32	−50	40	4.4
Inferior parietal	L	40	−44	−38	40	4.5
Fractal *n*-back						
Lingual gyrus	L	19	−24	−54	−4	4.4
Middle frontal	L	46	−40	26	24	4.1
Precentral	L	6	−28	−6	40	4.2
Precentral	R	6	36	−6	40	3.8
Inferior parietal	L	40	−36	−58	44	4.5

Note. *x*, *y*, and *z* are coordinates from Talairach and Tournoux (1988). *Z* scores represent peak activation in the cluster ($p < .05$, corrected). Hem = hemisphere (L = left, R = right); BA = Brodmann's areas.

Table 2

Local Maxima of Cerebral Blood Flow Change During 2-Back Minus 0-Back

Task and region	Hem	BA	*x*	*y*	*z*	*Z* score
Letter *n*-back						
Insula	R		36	18	0	4.5
Middle temporal	R	21/37	48	−50	4	4.8
Middle frontal	R	10	36	54	4	4.3
Middle frontal	R	9/46	44	34	28	5.3
Inferior frontal	L	44	−48	14	8	4.3
Inferior parietal	R	40	44	−42	40	5.1
	L	40	−52	−42	40	4.8
Fractal *n*-back						
Insula	L		−24	22	4	4.3
Insula	R		32	22	4	4.9
Middle frontal	L	46/10	−32	42	8	4.7
Middle frontal	R	46	40	30	24	5.1
Middle frontal	L	46	−40	26	24	4.5
Inferior frontal	L	44/6	−44	6	32	5.2
Anterior cingulate		32	0	26	40	4.8
Inferior parietal	R	40	40	−50	40	5.1
	L	40	−28	−54	40	5.4
Letter–fractal *n*-back						
Middle frontal	R	9/46	32	38	24	4.3

Note. *x*, *y*, and *z* are coordinates from Talairach and Tournoux (1988). *Z* scores represent peak activation in the cluster ($p < .05$, corrected). Hem = hemisphere (L = left, R = right); BA = Brodmann's areas.

Table 3

Local Maxima of Cerebral Blood Flow Change During 2-Back Minus 1-Back

Task and region	Hem	BA	*x*	*y*	*z*	*Z* score
Letter *n*-back						
Insula	R		28	26	8	4.4
Insula	L		−48	14	8	4.2
Middle frontal	R	10	36	46	20	4.4
Middle frontal	L	46	−36	26	24	4.5
Middle frontal	L	9	−44	6	36	4.3
Middle frontal	R	9	40	6	40	4.6
Thalamus	L		−12	−10	16	4.1
Anterior cingulate	R	32	4	22	36	4.2
Inferior parietal	R	40	44	−46	40	4.7
	L	40	−24	−58	40	4.6
Fractal *n*-back						
Middle frontal	L	10	−32	42	12	4.5
Middle frontal	R	46	44	30	24	4.8
Middle frontal	R	9	40	22	36	5.4
Inferior frontal	L	44/6	−44	2	32	4.8
Anterior cingulate	L	32	−4	26	36	5.2
Inferior parietal	L	40	−32	−54	40	4.0

Note. *x*, *y*, and *z* are coordinates from Talairach and Tournoux (1988). *Z* scores represent peak activation in the cluster ($p < .05$, corrected). Hem = Hemisphere (L = left, R = right); BA = Brodmann's areas.